Direct observation of intrinsic Josephson junction characteristics in electron-doped Sm2-xCexCuO4-delta

Kawakami, Tsuyoshi; Suzuki, Minoru

PHYSICAL REVIEW B **76**, 134503 (2007)

Direct observation of intrinsic Josephson junction characteristics in electron-doped $Sm_{2-x}Ce_xCuO_{4-\delta}$

Tsuyoshi Kawakami and Minoru Suzuki*
Department of Electronic Science and Engineering, Kyoto University, Kyotodaigaku-Katsura, Nishikyo-ku, Kyoto 615-8510, Japan
(Received 14 October 2006; revised manuscript received 11 July 2007; published 3 October 2007)

We have investigated the current-voltage (*CV*) characteristics of the intrinsic Josephson junctions (IJJs) in the electron-doped high-T_c superconductor $Sm_{2-x}Ce_xCuO_{4-\delta}$ by using a small mesa structure fabricated on a single crystal surface. It is found that multiple resistive branches, i.e., typical IJJ characteristics, are observed in the *CV* characteristics when the junction area of a mesa is 10 μm^2 or less. It is also found that a typical Josephson critical current density J_c is 7.5 kA/cm^2 at 4.2 K for T_c=20.7 K. The Josephson penetration depth is experimentally estimated to be 1.0–1.6 μm from the size dependence of J_c. Both J_c and T_c are found to decrease with the carrier doping level, as is found for hole-doped $Bi_2Sr_2CaCu_2O_{8+\delta}$ in the heavily overdoped region. These results are discussed in relation to the current locking in terms of the coupled Josephson junction stack model.

DOI: 10.1103/PhysRevB.76.134503 PACS number(s): 74.50.+r, 74.72.Jt

I. INTRODUCTION

Due to its layered structure and large anisotropy, a crystal of a high-T_c cuprate is generally regarded as a stack of tunnel Josephson junctions. These junctions are called intrinsic Josephson junctions (IJJs).[1,2] Since the IJJs are a crystal structure itself, the junction interfaces are atomically flat and clean, providing uniquely in high-T_c superconductors almost ideal tunneling-type Josephson junction characteristics. With these characteristics, the IJJs are employed in a wide variety of researches such as those into the macroscopic quantum tunneling,[3,4] the interlayer tunneling spectroscopy,[5,6] collective vortex motion,[7,8] and others.[9]

The current-voltage (*CV*) characteristics of the IJJs exhibit deep hysteresis and multiple resistive branches which correspond to the resistive states of the individual IJJs. Typical IJJ characteristics are usually observed in $Bi_2Sr_2CaCu_2O_{8+\delta}$ (BSCCO), in which the IJJ characteristics were observed for the first time,[1] and in $Tl_2Ba_2Ca_2Cu_3O_{10}$,[2,10] which has a crystal structure similar to BSCCO. These cuprates have a typical layered crystal structure and a significantly large anisotropy of ~100 or greater. $Hg_2Ba_2Ca_2Cu_3O_{10}$ has also a similar crystal structure and it was shown recently that this material also shows typical IJJ *CV* characteristics.[11]

On the other hand, in $YBa_2Cu_3O_{7-x}$ (YBCO), which has a crystal structure with a moderate anisotropy, the IJJ characteristics were observed only for a limited number of samples, which have a small junction area and a low carrier doping level (underdoped).[12–14] In $RuSr_2GdCu_2O_8$, which is crystallographically analogous to YBCO, multiple resistive branches similar to those for YBCO were also observed in the *CV* characteristics.[15] For $La_{2-x}Sr_xCuO_4$ crystals, multiple branches are not observed in the *CV* characteristics and the hysteresis is absent.[16] Thus *CV* characteristics of the IJJs are different among high-T_c cuprates, depending on the crystal structure, the magnitude of its anisotropy, and the sample dimensions. The appearance and disappearance of the multiple resistive branches, which correspond to the switching of individual IJJs, are closely related to the current locking phenomenon in a coupled Josephson junction stack.[17] The current locking is thought to occur through the inductive coupling between the junctions, that is, the Josephson coupling strength between the superconducting layers through the Josephson critical current density J_c and the penetration depth λ_J. Through J_c, on the other hand, the IJJ characteristics can be related to the inhomogeneity of the superconducting state, which is supposed recently.[18–20] Thus, the observation of the IJJ characteristics is important to understand the dynamics of a coupled Josephson junction array, and, in some cases, it is useful to probe into the inhomogeneous superconducting state of a cuprate.

Almost all the IJJ characteristics have been observed in hole-doped cuprates so far. Since the magnitudes of anisotropy and the Josephson plasma frequency for electron-doped cuprates are comparable with those for hole-doped cuprates, it is thought possible to observe the IJJ characteristics for electron-doped cuprates. In an earlier study, Schlenga *et al.*[21] observed the *CV* characteristics of the electron-doped high-T_c superconductor $Pr_{2-x}Ce_xCuO_{4+\delta}$ on a small platelet crystal. They observed the ac Josephson effect and several voltage steps in the *CV* characteristics, but not a multiple branch structure typical to IJJs. The present paper reports the direct observation of the IJJ characteristics and their multiple branch structure for the electron-doped cuprate $Sm_{2-x}Ce_xCuO_{4-\delta}$ (SCCO) by using a small mesa structure fabricated on a single crystal surface. It is also found that the *CV* characteristics exhibit multiple resistive branches, only when the lateral mesa width is less than a few micrometers. This result indicates that the crystal structure of SCCO functions as superconductor-insulator-superconductor (SIS)-type IJJs like that of BSCCO. We discuss the relationship between the mesa size and the appearance of the multiple resistive branches in terms of the current locking phenomenon.

In the present study, several physical parameters have also been determined. A typical value for J_c is found to be approximately 7.5 kA/cm^2 at 4.2 K for a SCCO mesa having a T_c of 20.7 K. From the size dependence of the Josephson critical current I_c, the value for λ_J is estimated to be 1.0–1.6 μm. This value is compared with the λ_J value calcu-

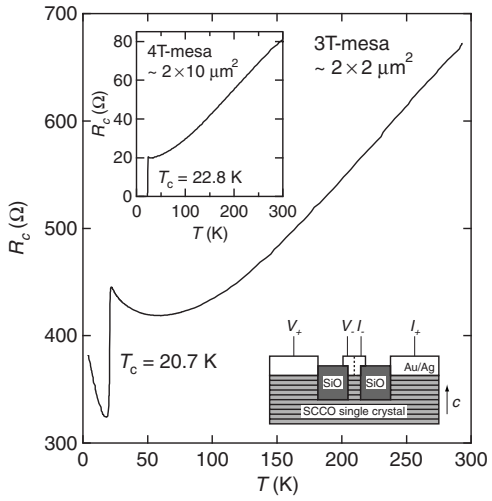

FIG. 1. Temperature dependence of the mesa resistance R_c for a SCCO 3T mesa 2×2 μm^2 wide and 36 nm thick. Excitation current is 1 μA. The top-left inset shows the T dependence of R_c for a SCCO 4T mesa 2×10 μm^2 wide and 30 nm thick at an excitation current of 5 μA. The bottom-right inset shows a schematic cross sectional view of the sample geometry (not to scale). For 4T mesas, a voltage terminal and a current terminal on top of a mesa are separated by a slit at the dashed line.

lated based on the coupled sine-Gordon equation. We also find that both J_c and T_c decreases monotonically with the carrier doping level. Finally, we discuss a possibility of the inhomogeneous superconducting state, which is suggested to exist in p-type cuprate superconductors.

II. SAMPLE FABRICATION

SCCO single crystals employed were grown by the self-flux method[22,23] using a turnover technique, which provided platelike single crystals with flux-free shiny surfaces. As-grown crystals were first annealed in flowing Ar at 945–950 °C for 15–20 h. Next, a Au(50 nm)/Ag(25 nm) double layer was evaporated on a crystal surface as a contact electrode, and then annealed in flowing Ar at 400 °C for 5 min to reduce the contact resistance. From these crystals, small mesa structures, as shown in the inset to Fig. 1, were fabricated on top of a crystal surface using a standard photolithography and an Ar ion milling technique.[5] The mesa thickness, typically 30 nm, was controlled by the milling time. The electrode configuration we employed is either of a three-terminal (3T) type or of a four-terminal (4T) type. The size of the 3T mesas ranges from 2×2 to 10×10 μm^2 in area and 36 nm in height, while that of the 4T mesas, which have two electrodes on the top, is approximately 2×10 μm^2 in area and 30 nm in height. These thicknesses of the mesas are much smaller than the averaged separation of the Sm_2O_3 impurity-phase epitaxial stacking layers, which was reported to be several hundred nanometers.[24] This implies that the mesas in the present study contain no such impurity layers and that the properties observed are inherent to SCCO. Since the spacing of the CuO_2 layers in SCCO is 0.60 nm, a mesa thickness of 30 nm corresponds to a stack of 50 IJJs.

III. RESULTS

Figure 1 shows the temperature T dependence of the mesa resistance R_c, i.e., the c-axis resistance, for a typical 3T mesa. The resistive superconducting transition is seen at a midpoint T_c of 20.7 K. Residual resistance seen below T_c is the contact resistance, which corresponds to a contact resistivity of 1×10^{-5} Ω cm^2 near T_c. This is the smallest contact resistivity attained in the present study. The c-axis resistivity ρ_c of the mesa obtained from R_c is 1.3 Ω cm just above T_c, which is nearly equal to the value obtained from a $Nd_{1.85}Ce_{0.15}CuO_4$ single crystal.[25] The inset of Fig. 1 shows a typical T dependence of R_c for a 4T mesa. The ρ_c value near T_c obtained from this 4T mesa coincides with that for the 3T mesa. The metallic behavior of ρ_c seen in the wide temperature range is commonly seen in the n-type cuprates.[22]

Figures 2(a)–2(c) show the IV characteristics for three different kinds of SCCO mesas: a 10×10 μm^2 3T mesa, a 2×2 μm^2 3T mesa, and a 2×10 μm^2 4T mesa. The samples in Figs. 2(b) and 2(c) are the same as those in Fig. 1. In Fig. 2(a), the IV curve exhibits neither hysteresis nor resistive branches, while in Fig. 2(b) the IV curve demonstrates small hysteresis and dozens of resistive branches. This is a typical difference seen in the IV characteristics when the mesas of different sizes are compared. Namely, the hysteresis and the resistive branches are observed when the mesa size is small. For 3T mesas, when the mesa area S is larger than a few μm^2 but smaller than 100 μm^2, the observed IV characteristics were occasionally intermediate ones between those in Fig. 2(a) and in Fig. 2(b). For example, the IV characteristics for a 5×5 μm^2 3T mesa exhibited small hysteresis and several nonhysteretic step. From the S dependence of the IV characteristics for more than a dozen of small mesa samples, it is concluded that the multiple resistive branches are observed only when S is less than approximately 10 μm^2.

In Fig. 2(c), on the other hand, the IV characteristics exhibit small hysteresis but no multiple resistive branches are seen. Although most of 4T mesas of the same size show similar IV characteristics, some of them occasionally exhibited a small steplike structure with an interval of 1–2 mV in the IV curve at low voltages. Similar IV characteristics were also observed for 5×5 μm^2 3T mesas. The relationship between the shape of the IV characteristics and S also holds in this case, indicating that the shape of the IV characteristics depends primarily on the mesa area, irrespective of electrode configurations. When the depth of the hysteresis is defined as $(I_c-I_r)/I_c$, as described in Fig. 2(c), the hysteresis for 2×10 μm^2 4T mesas ranged from 0% to 12%, as seen in the inset of Fig. 6(a). These values are significantly smaller than that of BSCCO, in which the hysteresis is much greater than 90%.

The dashed line in Fig. 2(c) corresponds to the resistance R_c at 24 K in the normal state. The IV curve approaches this line near ~40 mV, which value is still much smaller than 300 mV, the product of the superconducting gap voltage of $2\Delta/e=6$ mV (Ref. 26) and the number of junctions N of 50.

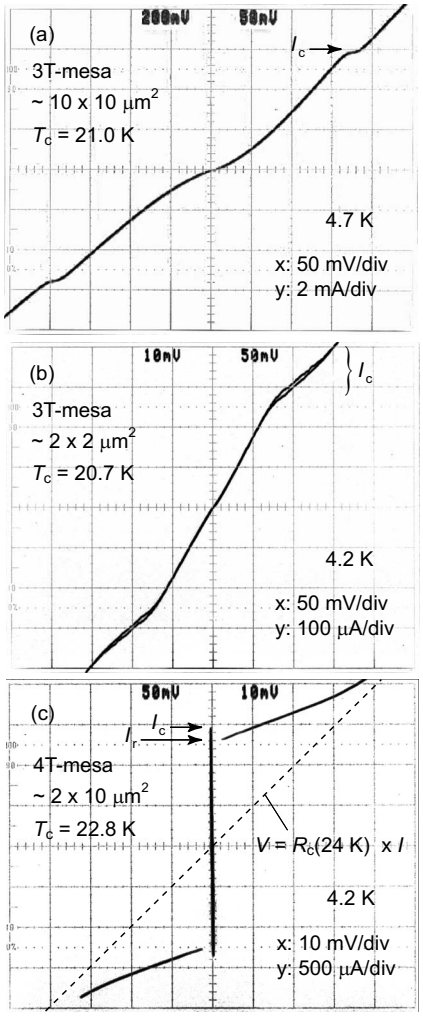

FIG. 2. *IV* characteristics for (a) 10×10 μm^2 3T mesa, (b) 2×2 μm^2 3T mesa, and (c) 2×10 μm^2 4T mesa. The dashed line in (c) indicates the resistance of $R_c=20$ Ω at 24 K. I_r in (c) indicates the return current, below which the junction switches to the zero-voltage state.

Even if we take into account the fact that the interval of the resistive branches is usually much smaller than $2\Delta/e$ by a factor of 1/4 to 1/3, as in the case of the IJJs in BSCCO, the value of such is not sufficient to explain the above value of 40 mV. If we further take into account the presence of the pseudogap,[27] which causes an increase in the normal state resistivity by a factor of as large as 2 below T_c, then the inclination of the dashed line in Fig. 2(c) is reduced to its half and the *IV* characteristics may turn out consistent with the usual tunneling model. It is also conceivable that the IJJs in SCCO crystals are accompanied by a small amount of a shunting resistance, which also reduces the interval of the resistive branches. The *IV* characteristics in Fig. 2(c) can be partly explained in terms of such a shunting resistance.

Figure 3 shows an enlarged view of the *IV* characteristics in Fig. 2(b) in the positive voltage range for the 2×2 μm^2 3T mesa at 4.2 K. In this measurement, an Ohmic resistive component comparable to the contact resistance was subtracted by using a differential circuitry. The distortion from

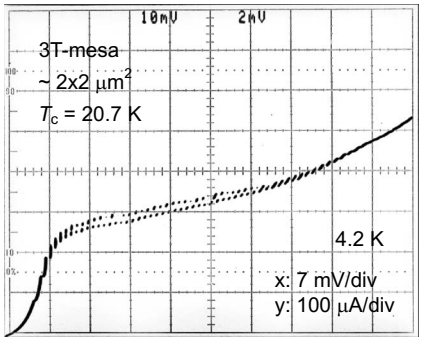

FIG. 3. The positive voltage part of the *IV* characteristics at 4.2 K for the 2×2 μm^2 3T mesa in Fig. 2(b). The characteristics were observed by subtracting the Ohmic resistive component of 250 Ω using a differential circuitry to remove influence of the contact resistance.

the linearity near the origin (bottom-left corner) is due to the contact resistance. The *IV* characteristic shows clearly the resistive branches counting approximately 60, which coincides with N, the number of the IJJs in the mesa. This agreement indicates that these resistive branches derive from the IJJs naturally built in the SCCO crystal structure like in the case for *p*-type BSCCO, and not from epitaxial stacking faults such as Sm_2O_3.[24] The regular resistive branches are seen at a constant voltage interval V_c of 1.0 mV, which is by a factor of approximately 1/6 smaller than the superconducting gap $2\Delta/e$ for *n*-type $Pr_{1.85}Ce_{0.15}CuO_4$ and $Nd_{1.85}Ce_{0.15}CuO_4$.[26] Furthermore, the value for $V_c/(2\Delta/e)$ is much smaller than that of ~1/3 for BSCCO.[28] The depth of the hysteresis is 10.3% at the most, which value is significantly smaller than that for BSCCO. As for the maximum Josephson current I_c for individual junctions for the sample in Fig. 3, the values are distributed from 150 to 450 μA. However, most of the junctions have an I_c of 250–350 μA in the 10–40 mV range. These values are averaged to obtain the value of $I_c=300$ μA. From this, the Josephson critical current density $J_c=I_c/S$ is obtained to be approximately 7.5 kA/cm^2 for this sample. The values for J_c were nearly the same for samples with similar S and T_c values. The above value is an order of magnitude larger than that of BSCCO (Ref. 29) and a factor of 2 larger than that of underdoped YBCO.[14]

The observed values of J_c for IJJs in SCCO lie between 1.4 kA/cm^2 for slightly overdoped BSCCO (Ref. 29) at 5 K and 26 kA/cm^2 for LSCO ($x=0.09$) at 4.2 K.[30] A typical value for the Josephson plasma frequency $\omega_p/2\pi$ for the *n*-type cuprates is 230 GHz, which lies between 107 GHz for BSCCO (Ref. 31) and 600 GHz for LSCO ($x=0.10$).[32] These values are in qualitative agreement with the relationship $\omega_p^2=2eI_c/\hbar C$, where C is the capacitance of a junction, because if we assume that $\varepsilon/\varepsilon_0=10$, the values for $\omega_p/2\pi$ are calculated to be 135 GHz for slightly overdoped BSCCO, 200 GHz for SCCO, and 369 GHz for LSCO ($x=0.09$).

Figure 4 shows the T dependence of I_c for the 2×2 μm^2 3T mesa shown in Fig. 3. The solid curve represents the theoretical I_c-T for a SIS Josephson junction based

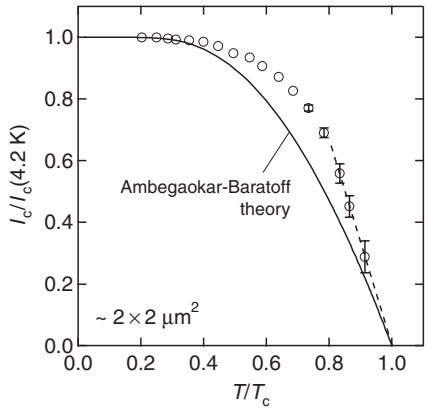

FIG. 4. T dependence of I_c for the 2×2 μm^2 3T mesa in Fig. 3. Values for I_c were obtained from the 13th resistive branch. The solid curve represents the Ambegaokar-Baratoff theory. The dashed line are guides to the eyes.

on the Ambegaokar-Baratoff (AB) theory.[33] The overall behavior demonstrates qualitatively a feature characteristic to a SIS-type Josephson junction. However, a slight deviation from the AB theory is seen in the T/T_c range of 0.4–0.9. The upward deviation like this is also seen for slightly overdoped BSCCO.[34] This presents a contrast with the I_c-T data for $RuSr_2GdCu_2O_8$,[15] underdoped YBCO,[13] and $La_{2-x}Sr_xCuO_4$,[16] in which only a little deviation is seen from the AB theory. The deviation of I_c-T from the theory may be related to the large junction effect at low temperatures. If the junction size is large compared with the Josephson penetration depth λ_J, I_c is suppressed appreciably at low temperatures because λ_J decreases as T decreases. This is discussed later in relation to the Josephson critical current density J_c.

Figure 5 shows the S dependence of I_c at 4.2–5 K for mesas whose T_c is 20–21 K. It is clearly seen that the I_c data start to deviate from the linear relationship when S exceeds ~10 μm^2. This result indicates that the value for the Josephson penetration depth λ_J is estimated to be 1.0–1.6 μm.[35] Thus, the I_c/S value obtained from a mesa of no larger than 2×10 μm^2 provides a good estimate for J_c.

It is known that the c-axis conductivity at 300 K, σ_c (300 K), is nearly proportional to the doping level in a doping range centered at the optimal doping.[18] Therefore, it is considered that the σ_c (300 K) dependence represents the doping dependence. Figures 6(a) and 6(b) show the plots of J_c vs σ_c (300 K) and those for T_c vs σ_c (300 K), respectively, for 2×10 μm^2 4T mesas and for 2×2 μm^2 3T mesas. In the sense mentioned above, Fig. 6 represents the doping dependence of J_c and T_c. From these plots, it is seen that J_c and T_c decreases monotonically with increasing doping level.[36] This doping dependence presents a sharp contrast with those for the BSCCO system, in which J_c increases significantly with increasing doping. This is interpreted in terms of the doping level of the superconducting region in the electron-doped cuprate system.[37] The details are discussed in the following section.

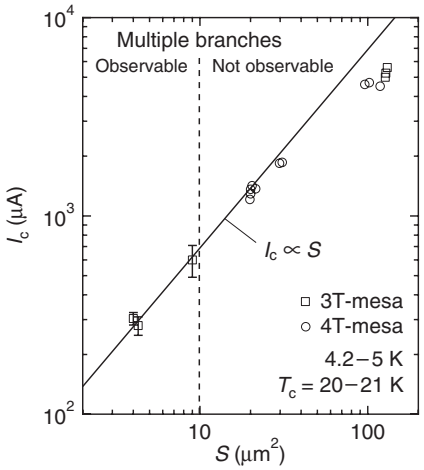

FIG. 5. S dependence of I_c for SCCO mesas with T_c = 20–21 K. The I_c values were measured at 4.2–5 K. The solid line represents the proportionality relationship between I_c and S. The dashed line represents the boundary for the appearance of multiple resistive branches. In the left side of the border, plots for I_c have error bars due to different I_c values among multiple resistive branches. The S values of ~4, ~9, ~20, ~30, and ~100 μm^2 in the plot correspond to the junction dimensions of 2×2, 3×3, 2×10, 3×10, and 10×10 μm^2, respectively.

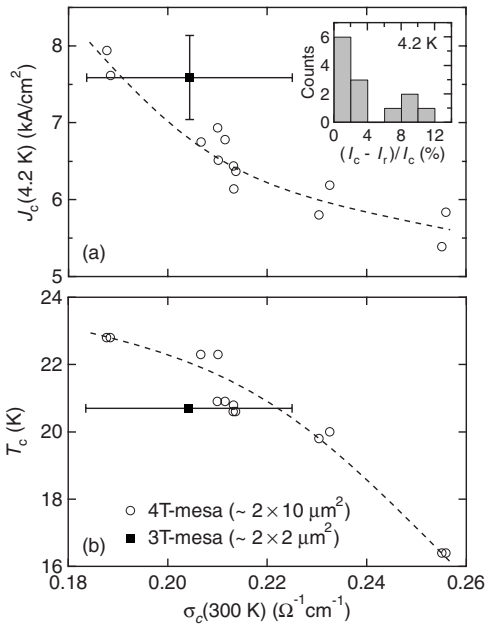

FIG. 6. Plots for (a) J_c (4.2 K) and (b) T_c as a function of σ_c (300 K). The filled symbols represent the data for the 2×2 μm^2 3T mesa in Fig. 3, while the open symbols represent the data for 2×10 μm^2 4T mesas. The σ_c (300 K) value for the 3T mesa is estimated by subtracting the extrapolated contact resistance at 300 K. The length of the vertical error bar represents the standard deviation of the J_c values. Dashed lines are guides to the eyes. The inset shows a histogram for the depth of hysteresis $(I_c-I_r)/I_c$ at 4.2 K for the 4T mesas. The depth of hysteresis showed no clear correlation with T_c.

IV. DISCUSSION

A. Mesa size dependence of the intrinsic Josephson junction characteristics

In the present study, it is found that the multiple resistive branches are seen in the *IV* characteristic only when the mesa area is less than 10 μm^2. It is known, on the other hand, that a mesa made of a BSCCO crystal shows multiple resistive branches with a large hysteresis in the *IV* characteristics even when the mesa is several tens of micrometer wide. The condition under which the multiple resistive branches are seen in the *IV* characteristics is related both to the presence of hysteresis and to the independent dynamic motion of each junction. If the *IV* characteristics exhibit no hysteresis or all the junctions are current locked and switch simultaneously, then the multiple resistive branches are not seen in the *IV* characteristics. In order to understand the present results, we need to rely on the following coupled sine-Gordon equation,[38,39] which describes the IJJs, as in Ref. 38.

$$\frac{d^2\gamma_n}{d\xi^2} = \frac{L^2}{\lambda_m^2} j_{z,n} - \frac{L^2}{\lambda_k^2}(j_{z,n-1} + j_{z,n+1}) - \left(\frac{1}{\lambda_m^2} - \frac{2}{\lambda_k^2}\right) L^2 j_{\mathrm{ext}},$$

$$\lambda_m^2 = \frac{\hbar}{2e\mu_0 t_{\mathrm{eff}} J_c}, \quad \lambda_k^2 = \frac{\hbar}{2e\mu_0 d_{\mathrm{eff}} J_c}, \tag{1}$$

where $t_{\mathrm{eff}}=t+2\lambda\coth(d/\lambda)$, $d_{\mathrm{eff}}=\lambda/\sinh(d/\lambda)$, $\lambda=d\lambda_{ab}/(d+t)$, t is the insulating layer thickness, d is the superconducting layer thickness, γ_n is the gauge-invariant phase between the $(n-1)$th and the nth superconducting layers, $j_{z,n}$ is the current between the $(n-1)$th and the nth superconducting layers normalized by J_c, L is the dimension of the junction along the x axis, $\xi=x/L$ is the normalized coordinate, and other notations are the same as in Ref. 38.

The coupling strength between adjacent junctions is determined by the second term in the right hand side of Eq. (1). Therefore, the ratio of the junction length L to λ_k determines the behavior of the dynamic motion. When $d,t \ll \lambda$, the relationship $\lambda_m \simeq \lambda_k$ holds. In this case, the Josephson penetration depth λ_J is equal to λ_m. From this relationship, it follows that when the ratio L/λ_k is larger than a certain value, all the junctions switch to the voltage state simultaneously, namely, the current locking (CL) phenomenon manifests itself. As numerically demonstrated by Goldobin and Ustinov,[17] this CL is a dynamic phenomenon brought about by the inductive coupling of long Josephson junctions. This is also supported experimentally on double junctions.[40] It is known that the IJJ resistive branches are observed for BSCCO in a much larger mesa sample than for SCCO. This fact implies that the value of λ_k for BSCCO is larger than that for SCCO. This is easily confirmed; if we use the values of $\lambda_{ab}=170$ nm,[41] $t=1.2$ nm, $d=0.3$ nm, and $J_c=500$ A/cm^2, we obtain the value of $\lambda_k=3.7$ μm for BSCCO, while if we use the values of $\lambda_{ab}=150$ nm,[42] $t=0.45$ nm, $d=0.15$ nm, and $J_c=7500$ A/cm^2, we obtain the value of $\lambda_k=0.68$ μm for SCCO. Thus, λ_k for SCCO is much smaller than that for BSCCO, so that the CL takes place in the IJJs of SCCO more easily than in BSCCO.

McCumber's parameter is represented by $\beta_c = 2eI_cR^2C/\hbar = 2eJ_c\rho_c^2\varepsilon_0\varepsilon_r(t+d)^2/\hbar t$. If we use the values of $\rho_c=1.33$ Ω cm, $\varepsilon_r=10$, $J_c=7.5\times10^3$ A/cm^2, $t=0.45$ nm, and $d=0.15$ nm, then we obtain $\beta_c=2.86$ for SCCO. Therefore, we can expect a small hysteresis in the *IV* characteristics of IJJs in SCCO. However, this value is larger than 1 by only a small amount so that it can change to less than 1 when ρ_c or J_c is decreased appreciably. The vicinity of β_c to 1 reflects the occasional disappearance of the hysteresis in the SCCO *IV* characteristics in the present experiments. On the other hand, it is easily seen that $\beta_c > 100$ for BSCCO and a large hysteresis is always expected in the *IV* characteristics of BSCCO IJJs. Since β_c is a parameter reflecting the capacitance of a Josephson junction, a large value for β_c probably favors the individual switching, where the charge is dynamically induced in the thin superconducting layers in the voltage state. It may be related to the fact that the multiple branch *IV* characteristics can be observed even in BSCCO mesas whose size is much larger than λ_J.

In the model described by Eq. (1), λ_m corresponds to λ_J, the Josephson penetration depth for a single junction. It is easily seen that $\lambda_m \simeq \lambda_J$ and $1/\lambda_k \simeq 0$ when $d \gg \lambda$. In the present case, $d \ll \lambda$, so that it holds that $\lambda_J \simeq \lambda_m \simeq \lambda_k = 0.68$ μm for SCCO using the values of $\lambda_{ab}=150$ nm and $J_c=7500$ A/cm^2. This value is smaller than the experimental value of 1.0–1.6 μm obtained from the S dependence of I_c by a factor of approximately 0.5. This may leave a possibility that the T dependence of I_c is influenced from the large junction effect, in which I_c is suppressed at low temperatures.

B. Doping dependence of J_c

As shown in Fig. 6(a), it is found that J_c decreases with increasing carrier doping level. According to the AB theory,[33] $J_c=\pi\Delta/2eR_N$ at $T=0$, where R_N is the normal tunneling resistance per unit area per junction. In the present study, R_N is nearly proportional to ρ_c, so that Fig. 6(a) combined with the AB theory implies that Δ decreases with increasing doping level. Since Fig. 6(b) indicates a decrease in T_c, the concomitant behavior of Δ and T_c is reasonable in light of the BCS theory. All these behaviors imply that the superconducting SCCO system is in the overdoped region. On the other hand, if we estimate the value for J_c using the values of $2\Delta=6$ meV, $R_NS=1.5$ Ω, $S=2\times3$ μm^2 ($\rho_c=1$ Ω cm), we obtain $J_c=7.85\times10^4$ A/cm^2, which is an order of magnitude larger than the observed value. The large difference between the AB theory and the experimental data as in the present study is also observed in the BSCCO system,[18,19] and is arguably regarded as evidence for the inhomogeneous superconducting state, where superconducting regions and nonsuperconducting ones are separated spatially on a fine scale. As in the underdoped BSCCO system, the present data may indicate the existence of the inhomogeneous superconducting state in the electron-doped SCCO system, even though the SCCO samples are in the overdoped region,[37] like in an overdoped BSCCO system, where inhomogeneous superconducting state is supposed to exist.[43] However, if we take into account that the present J_c values for the overdoped SCCO system are more than 2 orders of

magnitude larger than the J_c values for the underdoped BSCCO system, the above scenario needs further study to be convincing, in particular, on the doping dependence of J_c. A discrepancy of 1 order of magnitude in J_c can be accounted for in terms of different origins, which may include the large junction effect, *d*-wave symmetry of the superconducting order parameter, and others.[44,45]

V. CONCLUSIONS

We have observed the IJJ characteristics in the *n*-type SCCO system by using a small thin mesa structure. It is found that the multiple resistive branches, which reflects the individual switching of SIS-type IJJs, are observed in the *IV* characteristics only when the mesa area is below 10 μm^2. From the S dependence of I_c, λ_J is estimated to be 1–1.6 μm, which is compared with the theoretical estimate of 0.68 μm. In comparison with the case for the IJJs in the BSCCO system, it is found that the coupling strength of the IJJs in the SCCO system is greater than that in the BSCCO system. It is also found that J_c is approximately 7.5 kA/cm^2 at 4.2 K for a 2×2 μm^2 3T mesa with a T_c of 20.7 K. Both J_c and T_c are found to decrease with the carrier doping level, a behavior similar to the case for *p*-type BSCCO in the heavily overdoped region. The observed value for J_c is found to be an order of magnitude smaller than the theoretical estimate, which is indicative of the existence of the inhomogeneous superconducting state as a possible origin.

ACKNOWLEDGMENTS

The authors acknowledge useful discussions with T. Shibauchi. This work was partially supported by the 21st Century COE Program (Grant No. 14213201). T.K. was supported by the JSPS.

*Corresponding author; suzuki@kuee.kyoto-u.ac.jp

[1] R. Kleiner, F. Steinmeyer, G. Kunkel, and P. Müller, Phys. Rev. Lett. **68**, 2394 (1992).
[2] R. Kleiner and P. Müller, Phys. Rev. B **49**, 1327 (1994).
[3] K. Inomata, S. Sato, K. Nakajima, A. Tanaka, Y. Takano, H. B. Wang, M. Nagao, H. Hatano, and S. Kawabata, Phys. Rev. Lett. **95**, 107005 (2005).
[4] X. Y. Jin, J. Lisenfeld, Y. Koval, A. Lukashenko, A. V. Ustinov, and P. Müller, Phys. Rev. Lett. **96**, 177003 (2006).
[5] M. Suzuki, T. Watanabe, and A. Matsuda, Phys. Rev. Lett. **82**, 5361 (1999).
[6] V. M. Krasnov, A. Yurgens, D. Winkler, P. Delsing, and T. Claeson, Phys. Rev. Lett. **84**, 5860 (2000).
[7] S. Ooi, T. Mochiku, and K. Hirata, Phys. Rev. Lett. **89**, 247002 (2002).
[8] M. Tachiki, M. Iizuka, K. Minami, S. Tejima, and H. Nakamura, Phys. Rev. B **71**, 134515 (2005).
[9] A. A. Yurgens, Supercond. Sci. Technol. **13**, R85 (2000).
[10] K. Schlenga, G. Hechtfischer, R. Kleiner, W. Walkenhorst, P. Müller, H. L. Johnson, M. Veith, W. Brodkorb, and E. Steinbeiß, Phys. Rev. Lett. **76**, 4943 (1996).
[11] A. Ogawa, T. Sugano, H. Wakana, A. Kamitani, S. Adachi, Y. Tarutani, and K. Tanabe, Jpn. J. Appl. Phys., Part 2 **43**, L40 (2004).
[12] M. Rapp, A. Murk, R. Semerad, and W. Prusseit, Phys. Rev. Lett. **77**, 928 (1996).
[13] H. B. Wang, J. Chen, K. Nakajima, Y. Yamashita, P. H. Wu, T. Nishizaki, K. Shibata, and N. Kobayashi, Phys. Rev. B **61**, R14948 (2000).
[14] M. Nagao, T. Kawae, K. S. Yun, H. B. Wang, Y. Takano, T. Hatano, T. Yamashita, M. Tachiki, and H. Maeda, J. Appl. Phys. **98**, 073903 (2005).
[15] T. Nachtrab, D. Koelle, R. Kleiner, C. Bernhard, and C. T. Lin, Phys. Rev. Lett. **92**, 117001 (2004).
[16] Y. Mizugaki, Y. Uematsu, S. J. Kim, J. Chen, K. Nakajima, T. Yamashita, H. Sato, and M. Naito, J. Appl. Phys. **94**, 2534 (2003).
[17] E. Goldobin and A. V. Ustinov, Phys. Rev. B **59**, 11532 (1999).
[18] Y. Yamada, K. Anagawa, T. Shibauchi, T. Fujii, T. Watanabe, A. Matsuda, and M. Suzuki, Phys. Rev. B **68**, 054533 (2003).
[19] M. Suzuki, T. Hamatani, Y. Yamada, K. Anagawa, and T. Watanabe, IEEE Trans. Appl. Supercond. **15**, 189 (2005).
[20] Y. Yamada and M. Suzuki, Phys. Rev. B **74**, 054508 (2006).
[21] K. Schlenga, W. Biberacher, G. Hechtfischer, R. Kleiner, B. Schey, O. Waldmann, W. Walkenhorst, P. Müller, F. X. Regi, H. Savary, J. Schneck, M. Brinkmann, H. Bach, K. Westerholt, and G. Winkel, Physica C **235-240**, 3273 (1994).
[22] Y. Hidaka and M. Suzuki, Nature (London) **338**, 635 (1989).
[23] J. L. Peng, Z. Y. Li, and R. L. Greene, Physica C **177**, 79 (1991).
[24] P. K. Mang, S. Larochelle, A. Mehta, O. P. Vajk, A. S. Erickson, L. Lu, W. J. L. Buyers, A. F. Marshall, K. Prokes, and M. Greven, Phys. Rev. B **70**, 094507 (2004).
[25] H. J. Kang, P. Dai, J. W. Lynn, M. Matsuura, J. R. Thompson, S. C. Zhang, D. N. Argyriou, Y. Onose, and Y. Tokura, Nature (London) **423**, 522 (2003).
[26] S. Kleefisch, B. Welter, A. Marx, L. Alff, R. Gross, and M. Naito, Phys. Rev. B **63**, 100507(R) (2001).
[27] T. Kawakami, T. Shibauchi, Y. Terao, M. Suzuki, and L. Krusin-Elbaum, Phys. Rev. Lett. **95**, 017001 (2005).
[28] M. Suzuki, T. Watanabe, and A. Matsuda, IEEE Trans. Appl. Supercond. **9**, 4507 (1999).
[29] M. Suzuki, T. Watanabe, and A. Matsuda, Phys. Rev. Lett. **81**, 4248 (1998).
[30] Y. Y. Uematsu, N. Sasaki, Y. Mizugaki, K. Nakajima, T. Yamashita, S. Watauchi, and I. Tanaka, Physica C **362**, 290 (2001).
[31] T. Ichiguchi, Physica C **293**, 105 (1997).
[32] H. Shibata and T. Yamada, Physica C **293**, 191 (1997).
[33] V. Ambegaokar and A. Baratoff, Phys. Rev. Lett. **10**, 486 (1963).
[34] M. Suzuki, T. Watanabe, and A. Matsuda, IEEE Trans. Appl. Supercond. **9**, 4511 (1999).
[35] We employ a linear current-phase model of Barone *et al.* (Refs. 46 and 47), in which the Josephson current $J_c \sin\varphi$ is approximated by $J_c\chi\varphi$, where $\chi=1/2$. When the Josephson current flows perpendicular to the junction plane, this equation

together with the Maxwell equation leads to the ratio of the critical current to the junction area $I_c/S = (4\alpha\beta J_c\lambda_J^2/ab\chi^2)\tanh(a\chi/2\alpha\lambda_J)\tanh(b\chi/2\beta\lambda_J)$, where a and b are the side lengths of a rectangular junction, $S=ab$, α and β are constants with $\alpha^{-2}+\beta^{-2}=1$. For a square junction, where $a=b$ and $\alpha=\beta$, $I_c/S=0.9$ when $a/4\sqrt{2}\lambda_J=0.4$, leading to an estimate of $\lambda_J=1.4$ μm when $S=10$ μm^2. For a rectangular junction, where we assume that $|H_x/H_y|=a/b$ at corners $(\pm a/2, \pm b/2)$, then $\alpha/\beta=a/b$ and $I_c/S=0.9$ when $\sqrt{ab}/4\sqrt{\alpha\beta}\lambda_J=0.4$, leading to an estimate of $\lambda_J=1.22$ μm when $S=2\times 10$ μm^2 as reflected in Fig. 5. In the case of in-line type current flow, I_c/S starts to deviate when b is $2\lambda_J$ (Ref. 46), leading to an estimate of $\lambda_J=1.58$ μm when $a=b=\sqrt{10}$ μm^2, or an estimate of $\lambda_J=1.0$ μm when $a=10$ μm and $b=2$ μm. Thus, the result in Fig. 5 gives an estimate of $\lambda_J=1.0-1.6$ μm.

[36] In Fig. 6, the data for the 2×2 μm^2 3T mesa are also plotted, showing a slight deviation from the relationship for the 4T mesas. If we take into account the error due to the contact resistance, it is reasonably thought that the data for 3T mesas also fall on the same relationship.

[37] T. Kawakami, T. Shibauchi, Y. Terao, and M. Suzuki, Phys. Rev. B **74**, 144520 (2006).

[38] R. Kleiner, P. Müller, H. Kohlstedt, N. F. Pedersen, and S. Sakai, Phys. Rev. B **50**, 3942 (1994).

[39] S. Sakai, P. Bodin, and N. F. Pedersen, J. Appl. Phys. **73**, 2411 (1993).

[40] H. Yamamori, A. Fujimaki, Y. Takai, and H. Hayakawa, Jpn. J. Appl. Phys., Part 2 **33**, L846 (1994).

[41] M. Däumling and G. V. Chandrashekhar, Phys. Rev. B **46**, 6422 (1992).

[42] L. Fàbrega, J. Fontcuberta, B. Martínez, and S. Piñol, Phys. Rev. B **50**, 3256 (1994).

[43] K. Anagawa, T. Watanabe, and M. Suzuki, Phys. Rev. B **73**, 184512 (2006).

[44] S. Kashiwaya and Y. Tanaka, Rep. Prog. Phys. **63**, 1641 (2000).

[45] K. Maki and S. Haas, Phys. Rev. B **67**, 020510 (2003).

[46] A. Barone and G. Paternó, *Physics and Applications of the Josephson Effect* (Wiley, New York, 1982).

[47] A. Barone, W. J. Johnson, and R. Vaglio, J. Appl. Phys. **46**, 3628 (1975).